# HYDROACOUSTIC MONITORING OF THE SCOTIA SEA: AUTONOMOUS HYDROPHONE EXPERIMENT

Haruyoshi Matsumoto[1], DelWayne R. Bohnenstiehl[2], Robert P. Dziak[1], Minkyu Park[3], and Matthew J. Fowler[1]

National Oceanic and Atmospheric Administration[1], North Carolina State University[2], and the Korea Polar Research Institute[3]

Sponsored by the National Nuclear Security Administration

Award No. DE-AI52-08NA28654
Proposal No. BAA08-36

## ABSTRACT

Collaborating with the Korea Polar Research Institute, the National Oceanic and Atmospheric Administration and North Carolina State University began operating autonomous hydrophones (AUH) in the Scotia Sea waters near South Georgia Island in December 2007. An array consisting of six AUHs was successfully installed in an area of 86,000 $km^2$ to monitor the low-frequency acoustic events and ambient noise conditions for a period of about 13 months. Five of the AUHs were successfully recovered in January 2009; however, one instrument on the north side of the island was lost. All five of the recovered hydrophones recorded undisrupted 16-bit acoustic signals throughout the deployment, with four instruments sampled at 250 Hz and one instrument sampled at 1000 Hz. Our preliminary analysis reveals a bell-shaped seasonal ambient noise pattern of high in the fall and low in mid-winter, which is common to the partially ice-covered Southern Ocean. The seasonality of noise agrees with the formation of sea ice and ice break-up processes during the fall and the maximum sea ice extent during the winter in the region. During the first six months from December 2007 through June 2008, the five-AUH array located 200 seismic and 232 ice tremor events, while the National Earthquake Information Center (NEIC) registered 89 seismic events in the southwestern Atlantic Ocean region, indicative of the high sensitivity of the hydroacoustic method even at high latitudes. For shallow earthquakes along the Scotia subduction system, the AUH stations record a double peaked T-wave arrival packet. The first peak in T-wave energy is interpreted to be a secondary P-to-T conversion from the parabolic-shaped Scotia Volcanic Arc, which lies to the west of the epicenteral zone and to the east of the array. The second arrival corresponds to energy sourced in the vicinity of the seismically determined epicenter and is of larger amplitude and enriched in high frequencies relative to the first peak. The unique ambient noise and acoustic propagation environment of the Southern Ocean are discussed, and comparisons of seismic- and AUH-derived source locations are presented.

## OBJECTIVES

Monitoring underwater low-frequency sound is one of the critical components of the global nuclear explosions monitoring effort. The objective is to ensure that no nuclear weapon tests conducted in the ocean or near the surface above the ocean go undetected. One area where such a signal can be hidden from the eyes of the international community is the Scotia Sea. In the Scotia Sea propagation across the Antarctic Convergence Zone (ACZ) is poorly understood and the sound path to the International Monitoring system (IMS) hydrophones is partially or completely blocked by either the continents or islands and their associated seafloor ridge and arc systems.

The Scotia Sea is a small area of the southwest corner of the Atlantic Ocean surrounded by Tierra del Fuego and the Falkland, South Georgia, South Sandwich, and South Orkney islands and the Antarctic Peninsula. It is a tectonically complex area of marginal basins bordered by the Antarctic and South American plates, as well as the South Shetland, and Sandwich microplates. Due to the poor distribution of seismic stations and larger than 20 degree of separations between the stations (HOPE-South Georgia Island, EFI-East Falkland Islands and PMSA-Palmer Station), the minimum seismic detection threshold in the area has been close to $m_b$ 5.0. The hypocenter map from the International Seismic Center catalog (1964–1991) and the moment tensors of shallow centroids from Harvard's Centroid Moment Tensor (CMT) catalog (1977–1998) indicate the area is seismically active but is missing smaller events due to this sparse seismic distribution of monitoring stations in the area.

In contrast to global seismicity records, which suggest sparse seismicity, a regional seismic study of the South Shetland Island area based on both land-based and ocean-bottom seismometers (OBSs) shows a high level of local seismicity (Robertson Maurice et al., 2003). Our initial assessment of the hydrophone records from the 2005–2006 Bransfield deployment indicates a similar high rate of activity, with the detection of thousands of T-waves from seafloor earthquakes that cannot be associated with events in the global seismic catalog. These observations suggest a high occurrence rate of seismic events ($m_b > 3.0$) that can be utilized as natural sound sources for the propagation studies across the ACZ, with energy extending into the 30–45 Hz range.

Large icebergs are also known to produce hydroacoustic signals with distinct resonant characteristics similar to the harmonic tremor that often accompanies volcanic activity (e.g., Talandier et al., 2006; Chapp et al., 2005; Okal and MacAyeal, 2006). Ice tremors off Antarctica have been identified by the IMS hydrophone arrays as far away as the Northern Hemisphere and have been used to track the motion of the source icebergs. One ice-tremor signal in particular is estimated to have a source level of ~245 dB re $1\mu Pa|_{1m}$, equivalent to $m_b > 6$ earthquake. Icebergs breaking off in the Weddell Sea and drifting into the Scotia area should provide a significant number of these ice signal sources with known coordinates identified by QuickScat satellite imagery, which is provided by courtesy of the Center for Remote Sensing (CERS) at Brigham Young University (BYU).

By taking advantage of the high sensitivity of the hydroacoustic method (e.g., Fox et al., 2001; Bohnenstiehl et al., 2002; Dziak et al., 2004; Helffrich et al., 2006), our strategy was to install an acoustic array consisting of six AUHs for one year starting in December 2007 in the Scotia region and to analyze hydroacoustic activities in those areas after the recovery of the AUHs in early 2009. We expected that the arrays' low regional detection threshold of $m_b$ 2.0–3.0, due to the low attenuation properties of ocean-sound propagation and the 16-bit data resolution of the AUH data would afford a wide dynamic range of source levels, from the T-waves originating at the seafloor to the ice tremors from the surface.

Our goal is to provide a catalog of estimated hydroacoustic source locations with source levels and origin times, as well as associated arrival times and received levels. Located sound sources will be used to construct empirical blockage maps that can be compared with traditional line-of-sight blockage criteria or ray invariant approaches (e.g., Upton et al., 2006; Harben et al., 2003; Eggen and Dushaw, 2002).

## RESEARCH ACCOMPLISHED

Collaborating with the Korea Polar Research Institute, National Oceanic Atmospheric Administration, and North Carolina State University began with the operation of AUHs in the Scotia Sea region in December 2007. Five AUHs (M1–M5, white circles in Figure 1) were deployed from the R/V Yuzhmorgeologiya on the south side of the South Georgia Island during the first cruise. In April of 2008, the last AUH (M6) was deployed by a British Antarctic Survey ship, RRS JC Ross, at 280 nm NNE of the South Georgia Island. The array was optimally configured to

investigate sound propagation and interferences affected by the ACZ and land mass in the area, using the earthquakes and ice-related hydroacoustic events in the Scotia Sea as sound sources.

The recovery of hydrophones began in January of 2009 by the M/V Pharos SG. The operation went well, and five southern hydrophones (M1–M5) were successfully recovered. All five continuously recorded low-frequency acoustic signals (2–110 Hz) at a 250-Hz sampling rate for 13 months. However, recovery of the northern hydrophone, M6, became difficult due to weather conditions and ship schedules. A logistic decision was made to defer the M6 recovery to a later cruise. In April 2009, M/V Pharos SG sailed out again to recover the M6 mooring. Unfortunately, we found that at some point during the 1-year deployment, the top section (float and hydrophone) had been separated, leaving the rest of the mooring on the seafloor. The top 2000 m of mooring was made of a high-tension anti-strumming cable, and all the components were new. We were puzzled and disappointed at the loss of our instrument and data. Although there is a small chance that the instrument may wash ashore someday, our experience tells us that the chance is slim to none, so the instrument is deemed lost.

The lack of M6 data will limit our ability to assess the long-range effect interference by the ACZ and land mass to propagation of the sound northward. We will utilize data from all five recovered AUHs and from the IMS hydrophone from Ascension Island to compare the sound levels within the ACZ and outside of the ACZ. The five-hydrophone array encompasses a large area of approximately 80,000 $km^2$, with average element spacing of 280 km between 56$^o$S and 59$^o$S parallels. We are comparing the sound levels among the hydrophones and will assess the sound propagation within the ACZ and make comparisons with the model. We have completed locating the hydroacoustic events in the Scotia Sea area using the five hydrophones, and thus far we have detected 40% more earthquakes than the National Earthquake Information Center (NEIC) catalogs within the same period. Here we discuss the preliminary result our study of the 13 months of data.

**Preliminary Data Analysis**

All five Scotia Sea hydrophone spectrograms exhibit a bell-shaped seasonal ambient noise pattern, high in the fall and low in mid-winter. Figures 2a and 2b show 13-month-long spectrograms at the M3 and M5 sites, respectively. Throughout the deployment, the calls of fin whales (~18 Hz) were observed, the most frequent occurring during the spring and late fall. The calls of blue whales were also observed during from austral fall to early winter (April to June). These calls appeared as lines near ~30 Hz and ~90 Hz. A bell-shaped spectrogram (in light blue) was the result of wide-band noise generated by ice breaking up and forming during the fall. Such noise became quieter in late winter when the sea ice in the region reached its maximum extent. A minimum of three hydrophones are required to locate events. Although ice-related events are ubiquitous, source levels of the most ice events (e.g., sea ice breakups) are low and not all events are locatable. In comparisons of the M3 (Figure 2a) and M5 (Figure 2b) spectrograms, attenuation of sea ice noise is evident as a result of transmission loss from the ice edge to the hydrophone mooring.

The average clock shift at the end of the 13-month deployment was 1.9 seconds. The internal temperature sensors indicate that at the hydrophone mooring depth (~500 m), temperature was between –1.5 $^o$C and +2$^o$C, exhibiting small seasonal changes as a result of the strong influence of the Antarctic Circumpolar Current. Small temperature variations of the sea water would allow us a correction of timing by linear interpolatation and allow us to locate events within several a kilometer of resolution. Measurements taken with expendable bathythermographs during the cruise indicated that even during the austral summer, the propagation mode is surface limited in this region.

Figure 3 shows the epicenters of earthquakes derived from the AUH data during the first six months of deployment from December 29, 2007, through June 30, 2008. The green dots are the epicenters from National Earthquake Information Center (NEIC), which registered 89 earthquakes in its catalog. Our AUH array detected 200 earthquakes (yellow) during the same period. Approximately twice as many earthquakes were detected through the hydroacoustic method as a result of efficient sound propagation through the ocean, even in the area where the SOFAR sound channel is lacking. In addition, 232 ice tremor events (blue) were detected. Interestingly, almost no hydroacoustic events were located in the Weddell Sea. We think this is due not to the absence of events in this area but rather to the dissipation of sound energy by the dense sea ice coverage in the latitudes higher than 60$^o$S; the sound repeats reflections at the rugged sea ice surface and refractions, making the area seem to be an acoustically quieter spot. The southern-most edge of the locatable ice tremors (blue) approximately coincides with the sea ice edge during the winter of 2008–2009 (CERS database, BYU).

Another interesting finding so far is evidence of the Scotia Arc acting as an acoustic radiator for the hydroacoustic events occurring east of the volcanic chain (Figure 4). There is an early-arriving peak in the T-wave signals that appears to radiate from the shallow bathymetry of the arc after traveling as a P-wave over a considerable distance (~50–250 km). The larger-amplitude peak in the T-wave signal, which can arrive up to a couple minutes later, follows this and is sourced from near the NEIC epicenter (M 6.6 earthquake indicated by a yellow star, Figure 4). The early arrival can be more "diffuse," which may reflect the fact that the arc is a parabola. Figure 5 shows a plot of the time difference between T-wave peaks, which can be seen to scale with the distance to the crest of the arc, as measured along a great circle path between the NEIC epicenter and hydrophone.

Early studies of T-waves generated near arcs and islands described similar multi-peaked T-wave arrivals, which were assumed to also be related to local bathymetry near the epicenter (Johnson and Norris, 1968; Johnson et al., 1963). Using a bathymetric scattering model, de Groot-Hedlin and Orcutt (2001) later simulated the arrival patterns associated with a number of fore-arc events near Fox Island in the Aleutians. For such events, hydrophone stations in the Pacific typically record a symmetric first-arriving T-wave sourced in deep water near the epicenter and a later-arriving, slope-generated T-wave typically characterized by lower amplitudes and longer durations. There also have been reports of T- to P-wave conversions (Okal, 2001) and T-waves reflected by the continental mass (Hansen and Bowman, 2005); however, this is the first indication that P-waves may propagate through an island arc and be converted to T-waves on the opposite side, coupling into the water column by a down-slope conversion process. Moreover, we find that the second peak within the coda is still usable to locate the earthquake epicenter. For the Scotia Arc T-waves, the high-frequency component of the P-T conversed phase appears lost during propagation through the solid earth, leaving low-frequency energy (< 20 Hz) dominant (Figure 4). Similar effects have been documented in other trench environments for P-to-T converted phases that undergo long solid-earth propagation paths (e.g., de Groot-Hedlin and Orcutt, 2001; Obara, 2009).

## CONCLUSIONS AND RECOMMENDATIONS

After one year of deployment, five AUHs were recovered and one was lost during this experiment. The data quality of the five hydrophones is excellent, with negligible clock errors. The analysis of AUH data has begun, and so far the hydroacoustic events during the first three months have been located. As compared with the land-based teleseismic network, the hydroacoustic method has detected twice as many events. Ice-related hydroacoustic events are ubiquitous in this area and, as compared with the T-phase of earthquake origins, twice as many ice events were located. Ice being on the surface, using the ice sound rather than bottom-generated T-waves may be more practical for modeling the propagation of sound from a near-surface explosion. We have also found evidence of P-waves being converted to T-waves through the Scotia Island arc and, as the T-wave exits, the arc acting as an effective parabolic radiator, making the sound field more complex.

## ACKNOWLEDGEMENTS

We would like to express our gratitude to Drs. Chris Hindley and Anthony Martin of the British Antarctic Survey for carrying out the deployment of M6 in the international waters on the north side of the South Georgia Island. We also thank the officers and crew of the R/V Yuzhmorgeologiya and MV Pharos SG for deploying and recovering the hydrophones under unfavorable weather conditions. We are also indebted to the base commander Mr. Richard McKee on the Falkland Islands for help coordinating the hydrophone recovery operation. Data on iceberg position and sea ice extent were provided by the courtesy of CRS at BYU. Finally we express our deep gratitude to the Korea Polar Research Institute for providing the ship time and logistic support at the King Sejong Antarctic base.

## REFERENCES

Bohnenstiehl, D. R., M. Tolstoy, D. K. Smith, C. G. Fox, and R. P. Dziak (2002). Aftershocks sequences in the mid-ocean ridge environment: An analysis using hydroacoustic data, *Techtonophysics,* 354: 49–70.

Chapp, E., D. R. Bohnenstiehl, and M. Tolstoy (2005). Sound-channel observation of ice-generated tremor in the Indian Ocean," *Geochem. Geophys. Geosyst.*, 6: Q06003, doi:10.1029/2004GC000889.

de Groot-Hedlin, C. D. and J. A. Orcutt (2001). Excitation of T-phases by seafloor scattering, *J. Acoust. Soc. Am.*, 1944–1954.

Dziak, R. P., D. K. Smith, D. R. Bohnenstiehl, C. G. Fox, D. Desbruyeres, H. Matsumoto, M. Tolstoy, and D .J. Fornari (2004). Evidence of a recent magma dike intrusion at the slow spreading Lucky Strike segment, Mi-Atlantic Ridge, *J. Geophys. Res.* 109: B12102.

Eggen, C. and B. D. Dushaw (2002). A MATLAB driven GUI supporting computation of a two-dimensional field of view and simulation of propagation between points," MTS/IEEE Conference, October 29–31, 2002, Biloxi, MS, Abstract #612.

Fox, C. G., H. Matsumoto, and T-K. A. Lau (2001). Monitoring Pacific Ocean seismicity from an autonomous hydrophone array, *J. Geophys. Res.* 106: 4183–4206.

Hanson, J. A. and J. R. Bowman (2005). Methods for monitoring hydroacoustic events using direct and reflected T-waves in the Indian Ocean, *J. Geophys. Res.* 111: B02305.

Harben, O. E., E. Matzel, Z. Upton, and J. Pulli (2003). Hydroacoustic blockage calibration for discrimination, in *Proceedings of the 25th Seismic Research Review – Nuclear Explosion Monioring: Building the Knowledge Base*, LA-UR-03-6029, Vol. 1, pp. 524–529.

Helffrich G. et al. (2006). Hydroacoustic detection of volcanic ocean-island earthquakes, *Geophys. J. Int.* 167: 1529–1536.

Johnson, R. H. and R. A. Norris (1968). T-wave radiators in the western Aleutians, *Bull. Seismol. Soc. Am.* 58:1–10.

Johnson, R.H. and J. Northrup and R. Eppley (1963), Sources of Pacific T-phases, J. Geophys. Res. 68: 4251–4260.

Obara, K. and T. Maeda (2009). Reverse propagation of T waves from the Emperor seamount chain, *Geophy. Res. Let.* 36: L08304.

Okal, E. A., and D. R. MacAyeal (2006). Seismic recording on drifting icebergs: catching seismic waves, tsunamis and storms from Sumatra and elsewhere, S*eismol. Res. Let.* 77: 6, 659–671.

Okal, E. A., (2001). Converted T phases recorded on Hawaii from Polynesican nuclear test: A preliminary report, *Pure Appl. Geophys.* 158: 457–474.

Robertson Maurice, S. D., D. A.Wiens, P. J. Shore, E. Vera, and L. M. Dorman (2003). Seismicity and tectonics of the South Shetland Islands and Bransfield Strait from a regional broadband seismograph deployment, *J. Geophys. Res.* 108: B10, 2461.

Talandier, J. et al. (2006). Hydroacoustic signals generated by parked and drifting icebergs in the Southern Indian and Pacific Oceans, *Geophys. J. Inst.* 165: 817–834.

Upton, Z. et al. (2006). A reflected energy prediction model for long-range hydroacoustic reflection in the oceans, *J. Acoust. Soc. Am.* 119: 153–160.

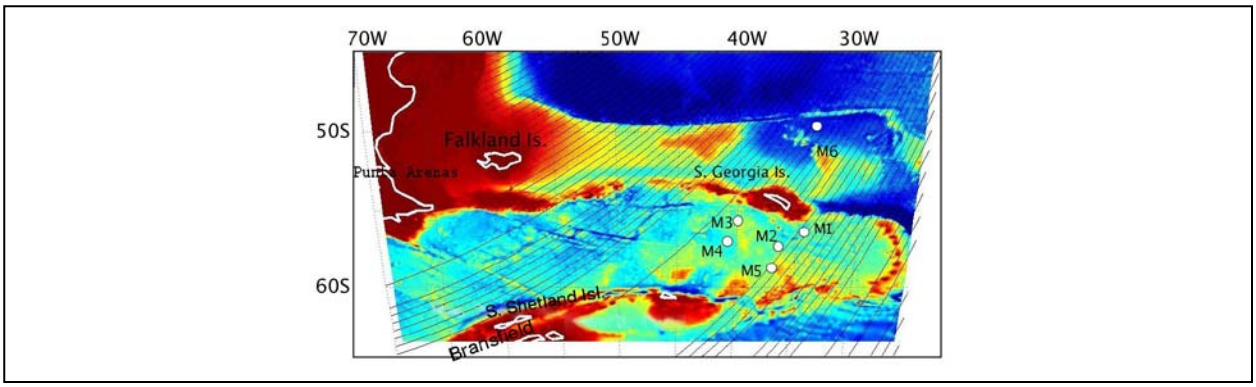


Figure 1. Hydrophone mooring locations.

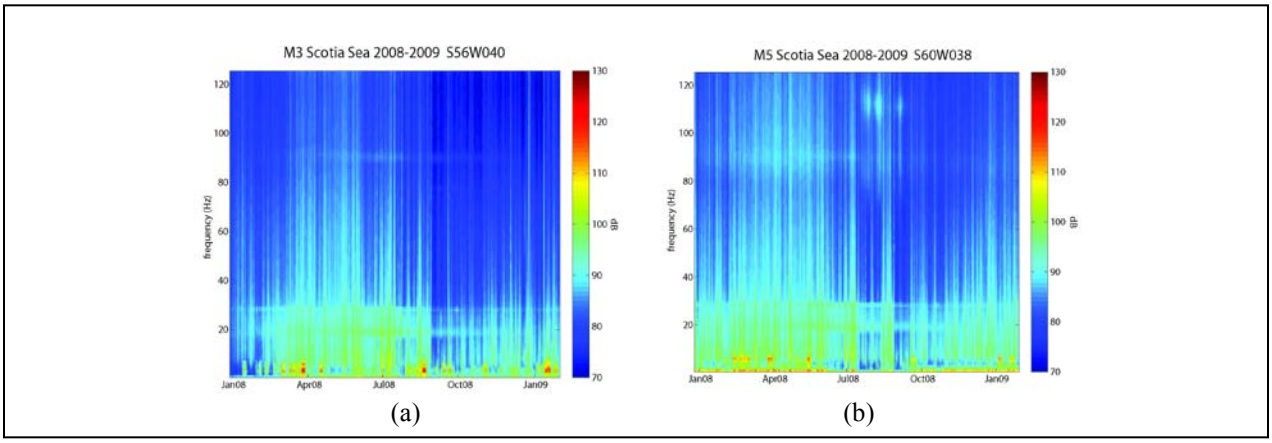


(a) (b)

**Figure 2. Seasonal noise spectrograms from December 2007 through January 2009. Spectrum levels are in dB relative to μPa$^2$/Hz. Spectrogram (a) is at the mooring M3, and (b) is at M5. The influence of ice noise, particularly in high frequencies, is much more pronounced at the southern hydrophone (M5), which was near the edge of sea ice during the 2008 austral winter.**

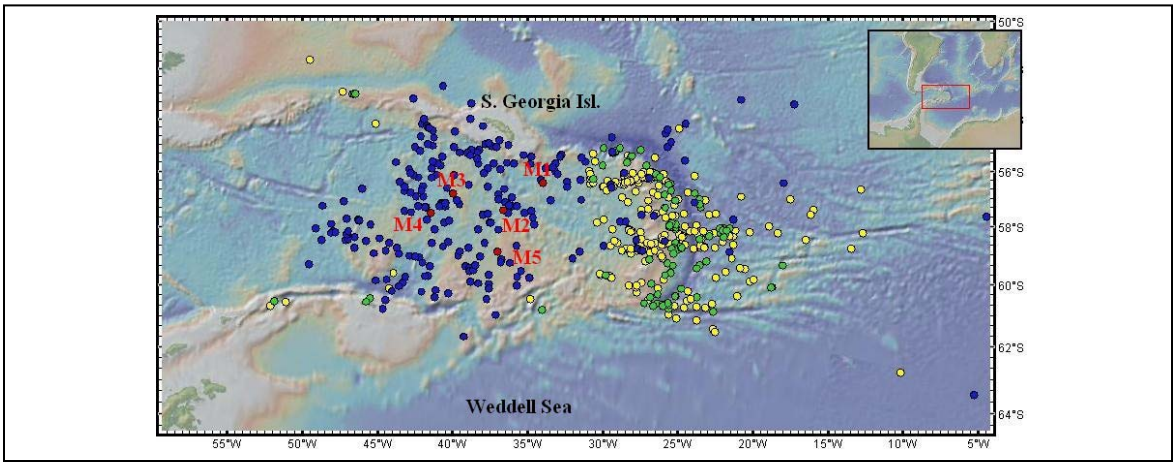


**Figure 3. Epicenters map derived from NEIC data (green) vs. AUH data (blue: ice, yellow: earthquake) from December 29, 2007, through June 30, 2008. Red circles indicate the mooring locations.**

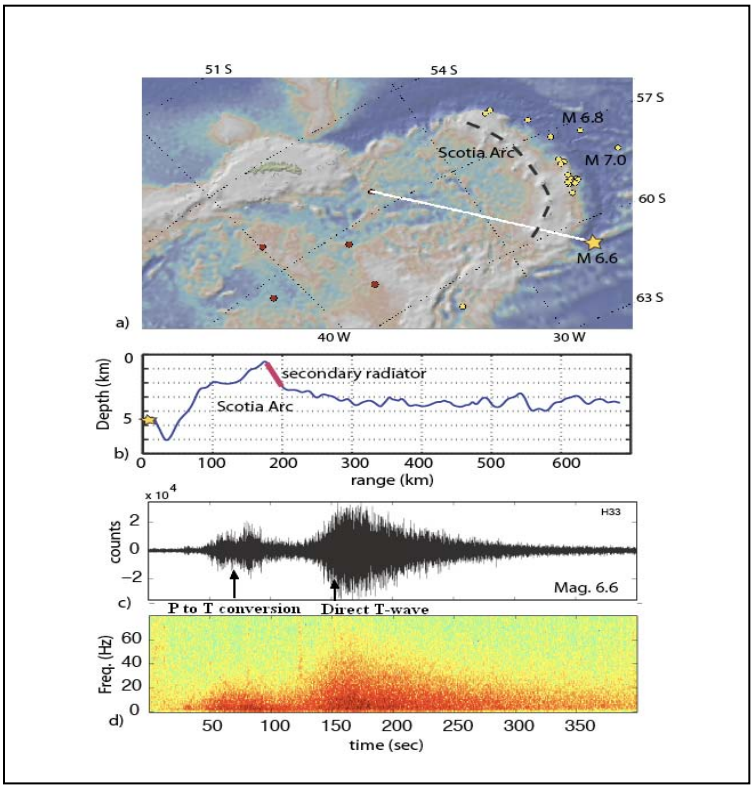


**Figure 4. (a) Map showing NEIC locations of the 28 earthquakes (yellow dots) identified as having double-peaked T-wave arrivals. These events lie to the east of the Scotia Arc, with the exception of one event behind a prominent ridge to the south. Shallow subduction interface events, which are closest to the volcanic arc, are the most common to exhibit this behavior. For events on the outer rise (more distant from the arc) the earlier-arriving phase is seen only for the events of greatest magnitude. (b) The bathymetric profile from source to receiver for the example arrival shown in (c) and (d). The first peak is typically a lower amplitude and deficient in high-frequency components, relative to the second. In this example, the time separation between the peaks is ~100 sec, consistent with its propagation as a P-wave along a 180-km-long path prior to conversion. Note that the larger, later-arriving phase is sourced from the deep-water epicenter and can still be used for location purposes.**

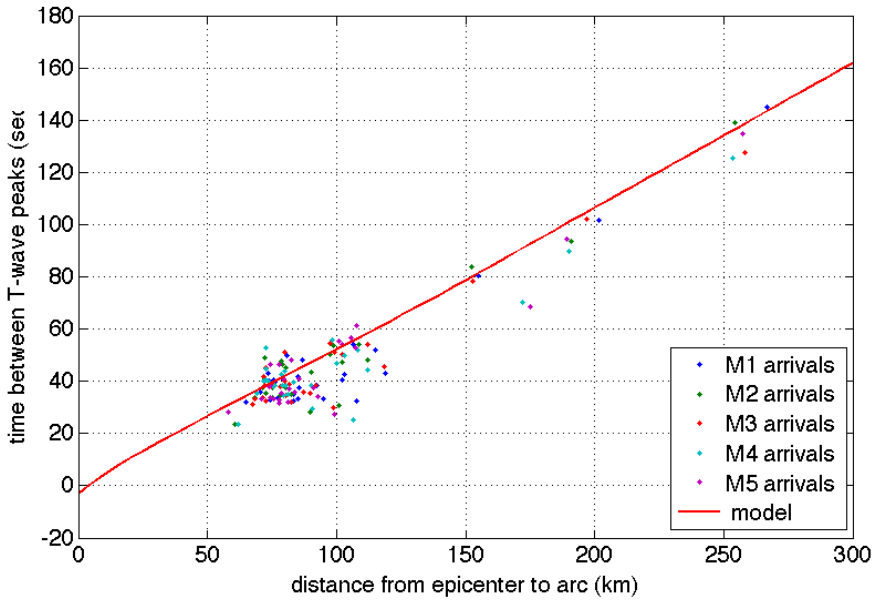


**Figure 5. Time difference between T-wave peaks within each arrival package plotted against the distance to the arc. Red line shows the predicted time difference, assuming P-wave propagation through an iasp91 model from a fixed 10-km-deep source and a T-wave velocity of 1.465 km/sec through the water column.**